Published in final edited form as:
Nat Chem Biol. 2012 October ; 8(10): 862–869. doi:10.1038/nchembio.1064.

The mechanism of acyl specific phospholipid remodeling by tafazzin

Michael Schlame[1,2], **Devrim Acehan**[3], **Bob Berno**[4], **Yang Xu**[1], **Salvatore Valvo**[3], **Mindong Ren**[2], **David L. Stokes**[3], and **Richard M. Epand**[4,5]

[1]Department of Anesthesiology, New York University School of Medicine, New York, New York, USA

[2]Department of Cell Biology, New York University School of Medicine, New York, New York, USA

[3]Skirball Institute, New York University School of Medicine, New York, New York, USA

[4]Department of Chemistry, McMaster University, Hamilton, Ontario, Canada

[5]Department of Biochemistry and Biomedical Sciences, McMaster University, Hamilton, Ontario, Canada

Abstract

Cardiolipin is a mitochondrial phospholipid with a characteristic acyl chain composition that depends on the function of tafazzin, a phospholipid-lysophospholipid transacylase, although the enzyme itself lacks acyl specificity. We incubated isolated tafazzin with various mixtures of phospholipids and lysophospholipids, characterized the lipid phase by ^{31}P-NMR, and measured newly formed molecular species by mass spectrometry. Significant transacylation was observed only in non-bilayer lipid aggregates and the substrate specificity was highly sensitive to the lipid phase. In particular, tetralinoleoyl-cardiolipin, a prototype molecular species, formed only under conditions that favor the inverted hexagonal phase. In isolated mitochondria, <1 percent of lipids participated in transacylations, suggesting that the action of tafazzin is limited to privileged lipid domains. We propose that tafazzin reacts with non-bilayer type lipid domains that occur in curved or hemifused membrane zones, and that acyl specificity is driven by the packing properties of these domains.

Tafazzin is a ubiquitous mitochondrial enzyme (1-4) that transfers acyl residues from phospholipids (PLs) to lysophospholipids (LPLs), producing new PLs and new LPLs in turn (5). It is a monotopic membrane protein that protrudes into the lipid phase without penetrating the entire membrane (3). The consequences of tafazzin deficiency, which include abnormal fatty acid composition of cardiolipin (CL), aberrant cristae morphology, and mitochondrial dysfunction leading to a human multisystem disease called Barth syndrome, suggest that the enzyme plays an important role in the biogenesis or the dynamics of mitochondria (1, 6-13).

Corresponding author: Michael Schlame, Departments of Anesthesiology and Cell Biology, New York University School of Medicine, 550 First Avenue, New York, NY 10016, USA. Tel.: +1 212 263 0648; michael.schlame@med.nyu.edu.

Author Contributions

M.S. conceived and designed the study, performed experiments, analyzed data, and wrote the paper. D.A., B.B., Y.X., and S.V. performed experiments, analyzed data, and interpreted the results. M.R. and D.L.S. gave technical support and conceptual advice. R.M.E. designed and performed experiments, analyzed data, and revised the manuscript.

Competing Financial Interest Statement

The authors declare no competing financial interests.

It has gradually become clear and it will be further expanded on in the present paper, that tafazzin can react with virtually all PL and LPL species (2, 5, 14). Thus, literally thousands of reactions are possible between all the PLs and LPLs present in mitochondrial membranes and the equilibrium constant close to 1 means that no direction can be assigned *a priori* to any specific transacylation. This unique situation raises a number of questions. First, it seems important to define which molecular species react with each other and what their products are as none of this can be inferred from known chemical properties. Second, it is puzzling why tafazzin does not equilibrate the fatty acid composition of all PLs because this is what one would expect thermodynamically as a result of free acyl exchange. Finally, it is difficult to envision how tafazzin brings about specific acyl patterns in CL, which is its most prominent effect (7-9, 15). Clearly, acyl specificity does not reside in the enzyme itself because transgenic expression of human tafazzin produces host-type rather than human-type CL (4, 16). Of course, it is possible that tafazzin acts in conjunction with another remodeling enzyme, such as a phospholipase, and it is the other enzyme that confers acyl specificity (17). Alternatively, acyl specificity may result from constraints imposed on the array of transacylation reactions by physical properties of the membrane, an idea we like to call "thermodynamic remodeling" (18). According to this idea, multiple transacylations will change the composition of molecular species until their combined free energy is minimal, in which case the composition is optimal for the specific state of the membrane. Magnitude and type of acyl transfer reactions will not only depend on the available substrate species but also on the physical properties of the membrane domain in which the reaction takes place. In the present paper, we tested this hypothesis by studying the transacylation equilibrium attained by isolated tafazzin in artificial PL/LPL aggregates.

Results

Endogenous tafazzin reacts only with a small pool of lipids in isolated mitochondria

Tafazzin is bound to mitochondrial membranes that also contain its substrates. In the absence of any barriers, one would therefore expect tafazzin to react with all mitochondrial PLs and LPLs. To determine the availability of endogenous substrate, we incubated isolated mitochondria with 1-^{14}C-palmitoyl-lysophosphatidylcholine (^{14}C-LPC). As shown before (2, 5), ^{14}C-LPC was converted into 1-^{14}C-palmitoyl-phosphatidylcholine (^{14}C-PC) by reacting with endogenous PLs: PL + ^{14}C-LPC → LPL + ^{14}C-PC. This reaction reached equilibrium after about 2 min although only a portion of the substrates had reacted at that time (Supplementary Fig. 1). At equilibrium, the ratio [^{14}C-PC]/[^{14}C-LPC] was <1 whereas the ratio of endogenous [PL]/[LPL] was >10, suggesting that only a subset of mitochondrial lipids participated in this reaction. Specifically, we estimated that < 1% of endogenous mitochondrial PLs were available for transacylation and, after measuring the amount of tafazzin by quantitative Western blot analysis (Supplementary Fig. 2), estimated that only about 700 PL molecules reacted per tafazzin molecule (Table 1). To test whether the amount of tafazzin was limiting the extent of the reaction, we over-expressed tafazzin in Sf9 insect cells. Although overexpression expanded the size of the reacting PL pool, the molar ratio of PL per tafazzin decreased, suggesting that the availability of transacylation-competent lipids became a limiting factor in the Sf9 expression system (Table 1). We concluded that tafazzin reacts only with a subpopulation of mitochondrial PLs and that some barrier must prevent complete transacylation of all PLs in the mitochondria.

Purified tafazzin reacts with PL/LPL micelles but not with monomers or bilayers

To define the physical conditions that promote PL-LPL transacylation, we studied the reaction of purified tafazzin with artificial membranes. Full-length Drosophila tafazzin (dTAZ) was expressed in E. coli as a construct fused to maltose-binding protein (MBP) and affinity purified on amylose resin as described (5). The enzyme was recovered as a micelle,

in which 79±12 molecules of Triton X-100 and 0.9±0.2 molecules of PL (either phosphatidylethanolamine, PE or phosphatidylglycerol, PG) were present per molecule of tafazzin (n=3). Triton did not inhibit the enzymatic activity of tafazzin (Supplementary Table 1). The purified enzyme bound to PC liposomes, reaching a maximal ratio of 1 molecule per 300 molecules of PC (Supplementary Fig. 3a), but it failed to react with the bulk of liposomal PC. This became clear when we incubated the enzyme with liposomes made of 20 nmol 16:0-18:2-PC and 1 nmol ^{14}C-16:0-LPC and allowed the reaction to attain equilibrium (x:y denotes an acyl residue with x carbon atoms and y double bonds). Instead of reaching a ^{14}C-PC/^{14}C-LPC ratio of 20:1, as one would expect in the equilibrium state, we measured a ^{14}C-PC/^{14}C-LPC ratio of 1:45, even though we estimated that >50 enzyme molecules were present per liposome. When we spun the lipid mixture after the reaction, we were surprised that ^{14}C-PC did not sediment with the liposomes but was mostly present in the supernatant (Supplementary Fig. 3b). This experiment suggested that although tafazzin bound to PC/LPC liposomes, the reaction took place between components of the 100,000 g supernatant, i.e. residual free enzyme and PC/LPC micelles. To further investigate the reaction of tafazzin, we switched from radiolabel to mass spectrometry because it allowed us to study a greater variety of substrates, to change substrate concentrations *ad libitum*, and to unequivocally identify the products. All molecular species resulting from a given PC-LPC reaction, including the two substrates and the two products could be detected and quantified in a single mass spectrum (Supplementary Fig. 4a), and the transfer of various acyl groups (14:0, 18:1, 18:2, 18:3) between lipids with various head groups (PC, PE, PG, CL, phosphatidylserine, PS) could be unequivocally documented (Supplementary Fig. 4b, c), confirming that tafazzin is a non-specific transacylase. In order to define the effect of the phase state, we measured transacylations at different PC:LPC ratios and determined the phase by magic angle spinning ^{31}P nuclear magnetic resonance (MAS ^{31}P NMR) spectroscopy. At high PC:LPC ratio, we calculated from the spinning side bands a large positive chemical shift anisotropy (CSA), which is characteristic of the bilayer state (19). At low PC:LPC ratio, we observed narrow symmetric lines without spinning side bands (CSA=0), which is characteristic of the micellar state (Table 2). The amount of transacylation product was negligible in the bilayer state but increased sharply when the substrate composition was shifted into the micellar state (Fig. 1a). When PC/LPC bilayers were converted from large multilamellar vesicles into small unilamellar vesicles, there was a minor increase in transacylation but it remained low compared to the micellar state (Supplementary Table 2). We also found that Triton X-100 increased transacylation when added to mixtures with high PC:LPC ratio but not when added to mixtures with low PC:LPC ratio, which supports the idea that tafazzin requires substrates to be presented as micelles (Supplementary Table 1). Finally, we studied the reaction of short-chain species that are in the micellar state at any PC:LPC ratio and compared it to even shorter species that are in the monomeric state. The data show that monomeric substrates (10:0-LPC/7:0-7:0-PC) produced little transacylation whereas micellar substrates (10:0-LPC/9:0-9:0-PC) produced high transacylation regardless of the PC/LPC ratio (Fig. 2a). In summary, these experiments indicate that transacylation by tafazzin is dependent on the physical state of substrates; the micellar aggregation form is strongly preferred over either lipid monomers or lipid bilayers.

Purified tafazzin reacts with non-bilayer assemblies of PE and CL

To determine whether other substrates show a similar dependence on the micellar state, we studied transacylations between LPC and either PE or CL. In contrast to PC/LPC, both PE/LPC and CL/LPC exhibited significant transacylation activity at high PL:LPL ratios (Fig. 1b, c). In order to characterize those states, we performed MAS ^{31}P NMR spectroscopy, which showed that PE formed a hexagonal phase with characteristic negative CSA, and that the phase state remained non-lamellar in the presence of low amounts of LPC (Table 2). The spectrum of CL, on the other hand, exhibited typical lamellar properties, i.e. the CSA was

positive. Upon addition of low amounts of LPC to CL (CL:LPC ratios of 9:1 or 8:2), the spectra suggested that non-lamellar structures were present as well (Supplementary Fig. 5;Table 2). Cryo-electron microscopy also supported the co-existence of lamellar and non-lamellar structures in CL/LPC (8:2) (Supplementary Fig. 6). In order to further explore the significance of non-bilayer phases, we added Ca^{2+}, which is known to convert CL into the inverted hexagonal state (20). Addition of Ca^{2+} to CL/LPC (8:2) caused lipids to precipitate out of solution and caused a significant increase in transacylation activity (Fig. 3a-c; Supplementary Table 2). For both CL and CL/LPC (8:2), the Ca^{2+} precipitates produced ^{31}P NMR lines with a characteristic hexagonal spinning side band pattern (Supplementary Fig. 5; Table 2). Ca^{2+} increased acyl transfer from 18:1-CL and 18:2-CL but not from 14:0-CL (Fig. 3b), further supporting the notion of an effect dependent on the formation of a hexagonal phase because 18:1-CL and 18:2-CL can adopt the hexagonal phase while 14:0-CL cannot (21). The effect of Ca^{2+} was specific for CL and was neither seen with negatively charged PG nor with zwitterionic PE (Fig. 3c) nor with zwitterionic PC (Supplementary Table 2). Interestingly, Ca^{2+} had the opposite effect on transacylation in the micellar phase, i.e. it suppressed transacylation in the presence of 80 percent LPC (Fig. 3a, b). We speculate that addition of Ca^{2+} to micellar CL/LPC mixtures caused sequestration of CL-Ca, which made it unavailable for transacylation. Overall, our data suggest that tafazzin reacts with substrates that form non-bilayer assemblies, such as hexagonal-type phases, certain kinds of micelles, and the type of non-lamellar structures present in CL/LPC or PE/LPC mixtures. It is important to point out that we observed similar effects when we used Sf9 cell mitochondria that over-expressed tafazzin instead of MBP-tagged purified tafazzin (Supplementary Fig. 7), indicating that the effects were due to the physical properties of the lipids but not the enzyme preparations.

The origin of specificity in the tafazzin reaction

To gain insight into how tafazzin discriminates among lipids in different phases, we studied the PC-LPC transacylation reaction in more detail. Kinetic analysis revealed that the reaction reached equilibrium in about 30 min (Fig. 2b) and that the amount of product present at equilibrium correlated with the enzyme concentration (Fig. 2c). The dependence of both catalytic rate and equilibrium product levels on tafazzin concentration, suggested that each enzyme molecule was restricted to a given substrate micelle. Turnover numbers, calculated from initial rates, were in the range of 1-2 molecules per min, which probably reflected the slow assembly of enzyme-substrate micelles rather than the true rate of catalysis. However, we are focusing here on equilibrium states, not on kinetic properties of the enzyme. Next, we examined a series of C18 PCs with varying degrees of unsaturation in mixed micelles with 14:0-LPC or 19:0-LPC. The amount of product formed at equilibrium increased with the number of double bonds in PC and it decreased with the chain length of LPC, suggesting that disorder in acyl chain packing promoted transacylation (Fig. 2d). When 18:0-18:1-PC was the acyl donor, we found that only 18:1 groups but not 18:0 groups were transferred regardless of whether 18:1 was bound to the sn-1 position or the sn-2 position (Fig. 2e). This experiment demonstrated the absence of positional specificity and raised the question why 18:0 was excluded from the reaction. Either the enzyme was incapable of transferring saturated acyl groups or the formation of disaturated products, such as 19:0-18:0-PC, was thermodynamically unfavorable. To specifically investigate the behavior of saturated acyl groups, we choose a mixture of deuterium-labeled 14:0d-14:0d-PC and 14:0-LPC, in which complete acyl exchange was expected by virtue of the fact that all acyl chains were 14:0. We found that deuterium-labeled 14:0 (14:0d) groups were transferred, resulting in formation of the partially deuterated species 14:0-14:0d-PC (Fig. 2f), which confirmed that the enzyme was active with saturated substrates. However, less than 5 percent (< 1 nmol) of 14:0d was transferred by the time the reaction attained equilibrium (Fig. 2b), which suggested that tafazzin did not have access to the entire

substrate pool and therefore failed to achieve full 14:0/14:0d exchange. We propose that the two substrates were partially segregated because disaturated PC and LPC have very different physical properties. For instance, 14:0-14:0-PC may not be sufficiently soluble in 14:0-LPC micelles and thus assemble separately in liposomes. Acyl transfer requires that both acyl donor and acceptor lipids are present in the vicinity of the enzyme and are not segregated into separate domains. Not only can immiscibility of substrates limit the transacylation, immiscibility of products can have the same effect, as suggested by the absence of 19:0-18:0-PC in Fig. 2e. In summary, our data suggest that transacylation is promoted by low packing order, presumably to facilitate PC-LPC mixing, and that phase separation of substrates may limit the reaction.

Reconstitution of acyl-specific CL remodeling in vitro

Since tafazzin is crucial for the fatty acid pattern of mitochondrial CL, we investigated whether the acyl remodeling of CL can be replicated in vitro and whether the lipid phase state has any effect on its specificity. To this end, we performed substrate competition experiments in CL/19:0-LPC mixtures containing different CL species. As expected, tafazzin formed 19:0-18:1-PC in the presence of 18:1-CL and 19:0-18:2-PC in the presence of 18:2-CL (Fig. 4a). When 18:1-CL and 18:2-CL were supplied together at a ratio of 1:1, about equal amounts of 19:0-18:1-PC and 19:0-18:2-PC were formed. However, when the same mixture was converted into the hexagonal phase, the transacylation product consisted almost entirely of 19:0-18:2-PC and only very little 19:0-18:1-PC, suggesting that the phase transition led to strong acyl specificity (Fig. 4a). Analogous competition experiments demonstrated that the hexagonal phase state generated strong preference for 18:1 over 14:0 and further increased the preference for 18:2 over 14:0 (Fig. 4b). Next, we created a model membrane that resembled the lipid composition of mitochondria, containing $(18:2)_2$-PC, $(18:1)_4$-CL, and small amounts of the LPL's 18:1-LPC and $(18:2)_3$-monolysocardiolipin (MLCL). This arrangement enabled a symmetric set of four competing transacylations, namely transfer of 18:2 from PC to either LPC or MLCL and transfer of 18:1 from CL to either LPC or MLCL (Fig. 5a). We varied the composition of the membrane from one that was dominated by PC to one that was dominated by CL, and we measured the composition of molecular species by mass spectrometry before and after incubation with purified tafazzin (Supplementary Table 3). In the absence of Ca^{2+}, small amounts of acyl groups were transferred in a tafazzin-dependent fashion and transacylations were restricted to two reactions, the transfer of 18:1 from CL to LPC and the transfer of 18:2 from PC to LPC (Fig. 5b). The ratio of the two reactions was roughly proportional to the concentrations of the corresponding acyl donors. Thus, under these conditions we did not find selectivity with respect to acyl groups but found strong selectivity with respect to the LPL head group (LPC>MLCL). The transacylation profile radically changed when we added Ca^{2+}, which increased the overall transacylation activity, elicited all four transacylation reactions, and induced a strong preference for 18:2 over 18:1 (Fig. 5b). Most importantly, Ca^{2+} triggered the formation of $(18:2)_4$-CL, the prototype species of mitochondrial CL. Addition of Ca^{2+} caused also alteration of the phase state of the CL/MLCL/LPC/PC mixture from one that was primarily lamellar to one that was primarily hexagonal, as demonstrated by the reversal of peak asymmetry in the ^{31}P NMR powder pattern (Fig. 5c). The effect of Ca^{2+} on the CL/MLCL/LPC/PC mixture is consistent with a previous report that Ca^{2+} induced a hexagonal phase not only in CL but also in CL/PC (22). Interestingly, the formation of $(18:2)_4$-CL was higher at a $(18:2)_2$-PC/$(18:1)_4$-CL ratio of 1:1 than at a $(18:2)_2$-PC/$(18:1)_4$-CL ratio of 7:1, suggesting that the propensity to adopt the hexagonal phase was more critical for $(18:2)_4$-CL formation than the abundance of 18:2 residues (Fig. 5b). Other transacylation products were identified as well, including 18:1-$(18:2)_3$-CL, $(18:1)_2$-PC, 18:1-18:2-PC, 18:2-LPC, and $(18:1)_3$-MLCL, and their rise was accompanied by the expected decrease in the concentration of substrates (Supplementary Table 3). In summary, we were able to mimic

CL remodeling in a simple lipid/tafazzin reaction system, in which formation of the signature species $(18:2)_4$-CL critically depended on the lipid phase state.

Discussion

The way tafazzin interacts with lipids and the mechanism by which it determines the acyl composition of cardiolipin have remained largely unexplained. In the present work we show that tafazzin reacts only with lipids that have low structural order and are not in the bilayer state. Acyl specificity does not arise on the basis of intrinsic enzymatic function but as a result of the physical characteristics of the lipids. This situation is in sharp contrast to that of some other enzymes, where acyl specificity is encoded by a conserved motif of the protein (23). From a mechanistic point of view, phase preferences of molecular species, which are based, in part, on their molecular size and shape (24), may naturally lead to lipid sorting and segregation and consequently to a selection of specific transacylation reactions. For example, bending of a membrane may cause significant disarray in the arrangement of bilayer-prone lipids, which can be relieved by transacylations producing curvature-prone lipid species, such as those that favor the hexagonal phase (Fig. 6). We show that both the extent and the substrate specificity of transacylations are directly affected by the lipid phase and that the physiologically relevant $(18:2)_4$-CL is formed by isolated tafazzin only under conditions promoting the inverted hexagonal state. While we cannot infer the precise structural arrangement of lipids in the vicinity of tafazzin and concede that the enzyme may alter the organization of lipids, the results demonstrate how lipids react with tafazzin if they have a natural tendency to adopt the hexagonal state. Both hexagonal and micellar phases can support transacylation activity and both are characterized by high curvature of the lipid-water interface, albeit with opposite signs, and by relatively disordered acyl chains (25, 26). We hypothesize that disorganized acyl chains allow for better mixing of PLs and LPLs, two types of molecules with conflicting packing geometries (24, 27), and that this is the reason why low packing order is a requirement for the tafazzin reaction.

It has been established that lipids of mitochondrial membranes are predominantly arranged in the bilayer state (28-30), which makes it difficult to envision how tafazzin is able to function in its native environment. However, mitochondria also contain local membrane regions in which the bilayer arrangement of lipids cannot prevail. For instance, hemifusion/hemifission sites must inevitably include non-bilayer lipids (31) and recent studies suggest that non-bilayer lipids of such sites undergo curvature-driven segregation (32) and interact with specific proteins like Drp1 and Bax (33). Furthermore, membrane regions with very high curvature such as those found at the edges of cristae or at cristae junctions (34) would be impossible without significant perturbation of the bilayer state. Any of these highly curved domains could potentially harbor the mitochondrial transacylation compartment. The idea that tafazzin acts only in privileged membrane domains, is consistent with our finding that only a small fraction of lipids reacts with tafazzin in isolated mitochondria and it explains the fact that the presence of tafazzin does not equalize the acyl composition of all mitochondrial lipids. Of course, complete CL remodeling can only occur under these presumptions if most if not all of mitochondrial CL comes temporarily into contact with the postulated domains.

In summary, we demonstrate that (i) tafazzin activity requires a perturbation of the bilayer state and (ii) transacylation specificity is determined by the physical properties of the membrane. These findings cast a new light on the biological function of tafazzin. If the enzyme does indeed exchange acyl groups in order to adapt the lipid composition to the shape of specific membrane domains, its actual role could be described as that of a “membrane chaperone” with lipid remodeling function (Fig. 6). Assembly of protein complexes, creation of membrane curvature, and mitochondrial fission and fusion, are all

expected to impose significant constraints on the overall arrangement of lipids. Such constraints can be mitigated by the action of tafazzin because the enzyme can quickly reshuffle acyl groups to establish an optimal lipid composition, thus reducing the energy cost. Importantly, the action of tafazzin is completely reversible, which allows for cyclic changes, such as fission and fusion or bending and flattening of the membrane. Thus, an important advantage conferred by tafazzin may be the flexibility of the lipid composition. In Barth syndrome, the absence of functional tafazzin leads to the reorganization of cristae, to local collapses of the inter-cristae space, and to accumulation of aggregated membranes (10), all being consistent with a disturbed dynamics of mitochondrial membranes as a result of reduced lipid flexibility.

Methods

Expression, purification and characterization of tafazzin

MBP-tagged full-length Drosophila tafazzin was expressed in E. coli strain BL21 using the pMAL-c2 vector. Cells were broken by sonication in the presence of 0.1% Triton X-100 and the enzyme was affinity-purified with amylase resin as described (5). The concentration of protein in the enzyme preparation was determined by the method of Lowry et al. (35). The concentration of Triton X-100 in the enzyme preparation was determined by UV absorbance at 274 nm, using a series of standard solutions for calibration. In order to analyze PLs present in the enzyme preparation, 10 mg MBP-tagged dTAZ were extracted with chloroform/methanol (36) and the extract was separated by thin-layer chromatography on silica gel 60 developed by chloroform-methanol-water (65-25-4). PL spots were identified by iodine vapor, digested in 70% perchloric acid at 180 °C, and quantified by the determination of phosphorus (37).

Transacylation reactions

Transacylation reactions were performed in triplicates. Results are given as mean values with standard error of mean. Lipids were purchased from Avanti Polar Lipids (Birmingham, Alabama), including deuterium-labeled PC that contained two perdeuterated myristoyl groups (14:0d-14:0d-PC). They were dried under a stream of nitrogen and dissolved in reaction buffer (0.05 M Tris, 0.5 mM EDTA, 10 mM β-mercaptoethanol, pH 7.4 at 37 °C) to yield a final concentration of 1 mM (100 nmol of total lipids per 100 μl per sample). In order to improve lipid dispersion, the mixtures were sonicated for 2 minutes in a sonicator bath. Unless indicated otherwise, incubations were started with 40 μg (0.48 nmol) MBP-tagged dTAZ and continued for 60 min at 37 °C. Reactions were stopped by addition of 2 ml methanol and 1 ml chloroform. Lipids were extracted (36), dried, re-dissolved in 50 μl chloroform-methanol (1:1), and analyzed by matrix-assisted laser desorption/ionization time-of-flight mass spectrometry (MALDI-TOF MS) as described (38). Samples were diluted 1:11 in 2-propanol-acetonitrile (3:2) and then mixed 1:1 with matrix solution containing 10 mg/ml 9-aminoacridine in 2-propanol-acetonitrile (3:2). One microliter was applied onto the target spots and MALDI-TOF MS was performed with a MALDI micro MX mass spectrometer from Waters. For the analysis of PC and LPC, the instrument was operated in positive ion mode and in reflectron mode and it was calibrated with polyethylene glycol. We typically acquired 10 laser shots per sub-spectrum and 100-200 sub-spectra per sample in a mass range from 400 to 2000 Da. Data were analyzed with MassLynx 4.1 software. We confirmed accurate PC quantification, originally demonstrated by Sun et al. (38), with several standard compounds. CL and MLCL were measured in a similar fashion, except that the instrument was operated in negative ion mode. Mass calibration was accomplished with a reference mixture of 14:0-lyso-PG (m/z=455.2415), $(18:1)_2$-PG (m/z=773.5338), $(18:2)_2$-PE (m/z=738.5079), and $(18:2)_4$-CL (m/z=1447.9650). In order to ensure accurate CL quantification, we first compared the signal intensities of various

molecular species that were available at known concentration, including 86:4-CL, 80:4-CL, 72:4-CL, 61:1-CL, 57:4-CL, 56:0-CL, and 54:6-MLCL. For species with 54 to 72 carbon atoms in the acyl moiety, we found equal signal intensities of the monoisotopic peaks after correction for the ^{13}C isotope abundance. Furthermore, we demonstrated a linear dependence of the signal intensity on the CL concentration within a range of 30 to 6,000 fmol per sample well.

^{31}P NMR

Samples were prepared for NMR analysis by mixing various PLs and LPLs to yield a total amount of 10 μmol. The solvents were removed under a stream of nitrogen and the lipid films were dried further under reduced pressure. Lipids were re-suspended by vigorous agitation in the same buffer used for transacylation reactions. The volume of buffer was 0.1 ml for MAS ^{31}P NMR measurements and 0.7 ml for static ^{31}P NMR measurements. $CaCl_2$ was added to some samples to give a 5-fold molar excess over CL. MAS ^{31}P NMR spectra were recorded on a Bruker AVANCE 500 spectrometer equipped with a standard bore 11.7 T magnet, giving a 202.45 MHz frequency for ^{31}P, and a 4 mm broadband tunable MAS probe. Samples were loaded into a 45 μl Kel-F insert of a 4 mm zirconium MAS/NMR rotor. Magic angle spinning was controlled using a Bruker model H2620 pneumatic MAS controller. The spin rate was typically set to 1200 Hz, but rates up to 3500 Hz were also employed in some samples. For static ^{31}P NMR analysis, samples were transferred to a Shigemi tube and spectra were recorded on a Bruker AVANCE 600 spectrometer (operating frequency for ^{31}P: 243 MHz), using a 5 mm solution state broadband observe probe. For both MAS and static spectra, the chemical shift scale was referenced to an external standard of 85% phosphoric acid and broadband proton decoupling was achieved with a WALTZ-16 decoupling type sequence at an applied field of approximately 3500 Hz. Spectra were recorded at 37 °C over a sweep width of 24 kHz. Raw spectra were recorded using 14K data points within an acquisition time of 0.3 s for static spectra and 8K data points within an acquisition time of 0.17 s for MAS spectra. About 3000 scans were acquired per spectrum for both static and MAS spectra. MAS spectra were analyzed using the Bruker Topspin solids line shape analysis routine (version 2.1) except for spectra with CSA=0, where Lorentzian lineshape deconvolution was employed. MAS spectra were simulated using the minimal number of components evident in the spectra.

Isolation of mitochondria and quantification of endogenous lipids and tafazzin

Mitochondria were isolated by differential centrifugation as described (5). The concentration of phospholipids was determined by measuring phosphorus in lipid extracts (37). The total amount of endogenous phospholipids in isolated mitochondria ranged from 250 to 300 nmol/mg protein. The amount of endogenous PLs reacting with tafazzin was determined by measuring ^{14}C-PC radioactivity after incubating mitochondria with ^{14}C-LPC for 15 min in order to reach equilibrium of the transacylation reaction ^{14}C-LPC + PL → ^{14}C-PC + LPL (see Supplementary Fig. 1). The amount of mitochondrial tafazzin was determined by quantitative Western blot analysis using reagents supplied by LiCor Biosciences (Lincoln, Nebraska). Western blotting was performed with a polyclonal rabbit antibody to Drosophila tafazzin (9) at a concentration of 1 μg/ml in Odyssey blocking buffer containing 0.01% Tween-20. LiCor GAR-IRDye800cw was used as the secondary antibody at a dilution of 1:15,000. Blots were analyzed by a LiCor 800 scanner in order to determine the fluorescence yield of the tafazzin bands. The fluorescence signal was calibrated with purified tafazzin.

Supplementary Material

Refer to Web version on PubMed Central for supplementary material.

Acknowledgments

We are grateful to Dr. B. De Kruijff for stimulating discussions. This work was supported by the Barth Syndrome Foundation, by the National Institutes of Health, and by the Canadian Natural Sciences and Engineering Research Council.

References

1. Ma L, Vaz FM, Gu Z, Wanders RJA, Greenberg ML. The human TAZ gene complements mitochondrial dysfunction in the yeast taz1Δ mutant. Implications for Barth syndrome. J. Biol. Chem. 2004; 279:44394–44399. [PubMed: 15304507]
2. Testet E, et al. Ypr140wp, 'the yeast tafazzin', displays a mitochondrial lysophosphatidylcholine (lyso-PC) acyltransferase activity related to triacylglycerol and mitochondrial lipid synthesis. Biochem. J. 2005; 387:617–626. [PubMed: 15588229]
3. Claypool SM, McCaffery JM, Koehler CM. Mitochondrial mislocalization and altered assembly of a cluster of Barth syndrome mutant tafazzins. J. Cell Biol. 2006; 174:379–390. [PubMed: 16880272]
4. Xu Y, et al. Characterization of tafazzin splice variants from humans and fruit flies. J. Biol. Chem. 2009; 284:29230–29239. [PubMed: 19700766]
5. Xu Y, Malhotra A, Ren M, Schlame M. The enzymatic function of tafazzin. J. Biol. Chem. 2006; 281:39217–39224. [PubMed: 17082194]
6. Bione A, et al. A novel X-linked gene, G4.5. is responsible for Barth syndrome. Nature Gen. 1996; 12:385–389.
7. Vreken P, et al. Defective remodeling of cardiolipin and phosphatidylglycerol in Barth syndrome. Biochem. Biophys. Res. Comm. 2000; 279:378–382. [PubMed: 11118295]
8. Gu Z, et al. Aberrant cardiolipin metabolism in the yeast taz1 mutant: A model for Barth syndrome. Mol. Microbiol. 2004; 51:149–158. [PubMed: 14651618]
9. Xu Y, et al. A Drosophila model of Barth syndrome. Proc. Natl. Acad. Sci. USA. 2006; 103:11584–11588. [PubMed: 16855048]
10. Acehan D, Xu Y, Stokes DL, Schlame M. Comparison of lymphoblast mitochondria from normal subjects and patients with Barth syndrome using electron microscopic tomography. Lab. Invest. 2007; 87:40–48. [PubMed: 17043667]
11. Claypool SM, Boontheung P, McCaffery JM, Loo JA, Koehler CM. The cardiolipin transacylase, tafazzin, associates with two distinct respiratory components providing insight into Barth syndrome. Mol. Biol. Cell. 2008; 19:5143–5155. [PubMed: 18799610]
12. Acehan D, et al. Cardiac and skeletal muscle defects in a mouse model of human Barth syndrome. J. Biol. Chem. 2011; 286:899–908. [PubMed: 21068380]
13. Acehan D, et al. Cardiolipin affects the supramolecular organization of ATP synthase in mitochondria. Biophys. J. 2011; 100:2184–2192. [PubMed: 21539786]
14. Malhotra A, Xu Y, Ren M, Schlame M. Formation of molecular species of mitochondrial cardiolipin. 1 A novel transacylation mechanism to shuttle fatty acids between sn-1 and sn-2 positions of multiple phospholipid species. Biochim. Biophys. Acta. 2009; 1791:314–320. [PubMed: 19416660]
15. Schlame M, et al. Deficiency of tetralinoleoyl-cardiolipin in Barth syndrome. Ann. Neurol. 2002; 51:634–637. [PubMed: 12112112]
16. Vaz FM, Houtkooper RH, Valianpour F, Barth PG, Wanders RJA. Only one splice variant of the human TAZ gene encodes a functional protein with a role in cardiolipin metabolism. J. Biol. Chem. 2003; 278:43089–43094. [PubMed: 12930833]
17. Beranek A, et al. Identification of a cardiolipin-specific phospholipase encoded by the gene CLD1 (YGR110W) in yeast. J. Biol. Chem. 2009; 284:11572–11578. [PubMed: 19244244]
18. Schlame M. Formation of molecular species of mitochondrial cardiolipin. 2 A mathematical model of pattern formation by phospholipid transacylation. Biochim. Biophys. Acta. 2009; 1791:321–325. [PubMed: 19416646]

19. McLaughlin AC, Cullis PR, Berden JA, Richards RE. ^{31}P NMR of phospholipid membranes: Effects of chemical shift anisotropy at high magnetic field strengths. J. Magn. Res. 1975; 20:146–165.
20. Rand RP, Sengupta S. Cardiolipin forms hexagonal structures with divalent cations. Biochim. Biophys. Acta. 1972; 255:484–492. [PubMed: 4333431]
21. Sankaram MB, Powell GL, Marsh D. Effect of acyl chain composition on salt-induced lamellar to inverted hexagonal phase transitions in cardiolipin. Biochim. Biophys. Acta. 1989; 980:389–392. [PubMed: 2713413]
22. De Kruijff B, et al. Further aspects of the Ca^{2+}-dependent polymorphism of bovine heart cardiolipin. Biochim. Biophys. Acta. 1982; 693:1–12. [PubMed: 7150583]
23. Shulga YV, Topham MK, Epand RM. Study of arachidonoyl specificity in two enzymes of the PI cycle. J. Mol. Biol. 2011; 409:101–112. [PubMed: 21477596]
24. Israelachvili JN, Marcelja S, Horn RG. Physical principles of membrane organization. Q. Rev. Biophys. 1980; 13:121–200. [PubMed: 7015403]
25. Thurmond RL, Lindblom G, Brown MF. Curvature, order, and dynamics of lipid hexagonal phases studied by deuterium NMR spectroscopy. Biochemistry. 1993; 32:5394–5410. [PubMed: 8499443]
26. Otten D, Löbbecke L, Beyer K. Stages of the bilayer-micelle transition in the system phosphatidylcholine-$C_{12}E_8$ as studied by deuterium- and phosphorous-NMR, light scattering, and calorimetry. Biophys. J. 1995; 68:584–597. [PubMed: 7696511]
27. Cullis PR, deKruijff B. Lipid polymorphism and the functional roles of lipids in biological membranes. Biochim. Biophys. Acta. 1979; 559:399–420. [PubMed: 391283]
28. Cullis PR, et al. Structural properties of phospholipids in the rat liver inner mitochondrial membrane. Biochim. Biophys. Acta. 1980; 600:625–635. [PubMed: 7407135]
29. DeKruijff B, Nayar R, Cullis PR. 31P-NMR studies on phospholipid structure in membranes of intact, functionally-active rat liver mitochondria. Biochim. Biophys. Acta. 1982; 684:47–52. [PubMed: 7055555]
30. Nicolay K, van der Neut R, Fok JJ, deKruijff B. Effect of adriamycin on lipid polymorphism in cardiolipin-containing model and mitochondrial membranes. Biochim. Biophys. Acta. 1985; 819:66–65. [PubMed: 4041452]
31. Chernomordik LV, Kozlov MM. Mechanics of membrane fusion. Nature Struct. Mol. Biol. 2008; 15:675–683. [PubMed: 18596814]
32. Nishizawa M, Nishizawa K. Curvature-driven lipid sorting: Coarse-grained dynamics simulation of a membrane mimicking a hemifusion intermediate. J. Biophys. Chem. 2010; 1:86–95.
33. Montessuit S, et al. Membrane remodeling induced by the dynamin-related protein Drp1 stimulates Bax oligomerization. Cell. 2010; 142:889–901. [PubMed: 20850011]
34. Davies KM, et al. Macromolecular organization of ATP synthase and complex I in whole mitochondria. Proc. Natl. Acad. Sci. USA. 2011; 108:14121–14126. [PubMed: 21836051]
35. Lowry OH, Rosebrough NJ, Farr AL, Randall RJ. Protein measurement with Folin phenol reagent. J. Biol. Chem. 1951; 193:265–275. [PubMed: 14907713]
36. Bligh EG, Dyer WJ. A rapid method of total lipid extraction and purification. Can. J. Biochem. Physiol. 1959; 37:911–917. [PubMed: 13671378]
37. Cook AM, Daughton CG. Total phosphorus determination by spectrophotometry. Meth. Enzymol. 1981; 72:292–295. [PubMed: 7311835]
38. Sun G, et al. Matrix-assisted laser desorption/ionization time-of-flight mass spectrometric analysis of cellular glycerophospholipids enabled by multiplexed solvent dependent analyte-matrix interactions. Anal. Chem. 2008; 80:7576–7585. [PubMed: 18767869]

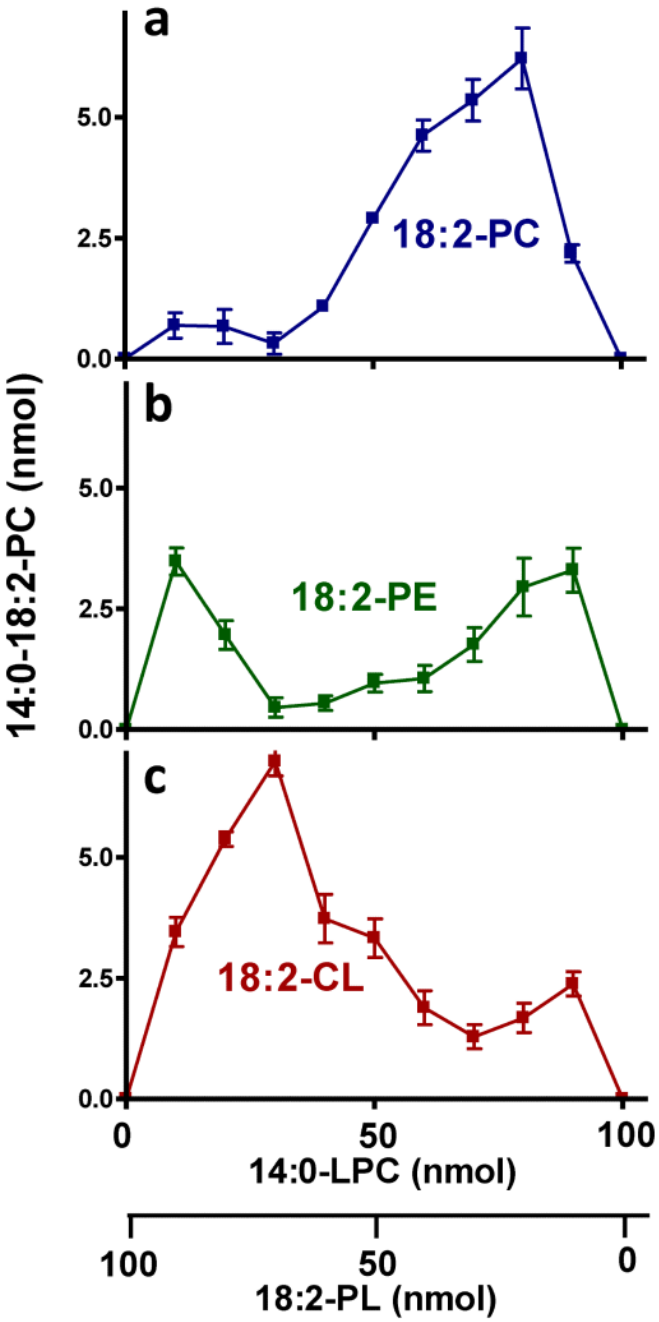

Figure 1. Transacylations are affected by the PL/LPL ratio

Incubations were performed with purified tafazzin, 14:0-LPC, and the indicated PL. The PL/LPC ratio was varied while maintaining a total amount of PL+LPC of 100 nmol. PLs included 18:2-18:2-PC, 18:2-18:2-PE, and bovine heart CL. The amount of transacylation product formed depends on the PL/LPC ratio.

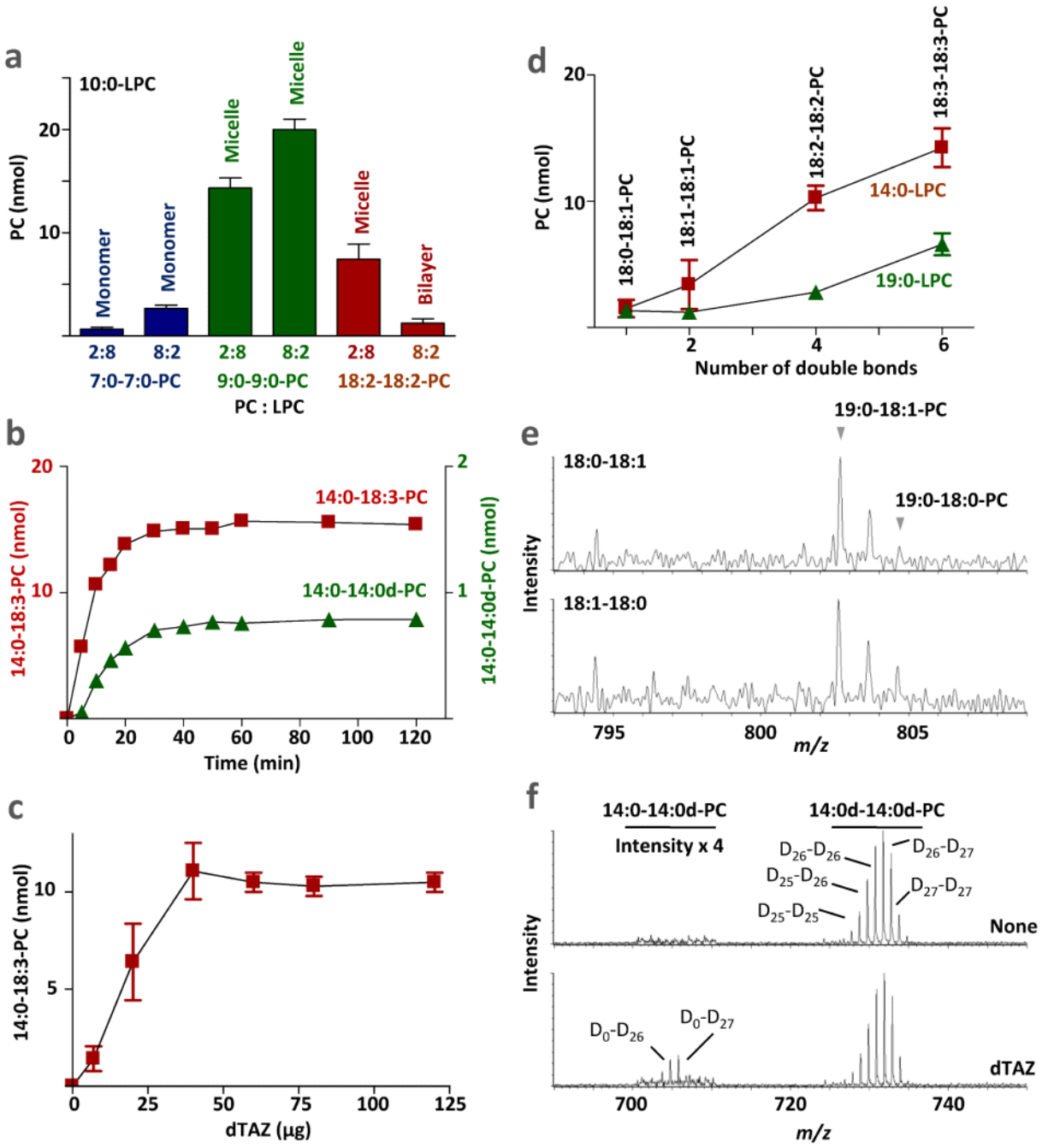

Figure 2. Transacylations in PC/LPC mixtures

(**a**) Tafazzin reacts with micelles but not with monomers or bilayers. Different PC species were incubated with 10:0-LPC at the indicated PC:LPC ratio and the concentrations of new PC species were determined. Based on their critical micellar concentration, 10:0-LPC/7:0-7:0-PC mixtures are predicted to form monomers, 10:0-LPC/9:0-9:0-PC mixtures are predicted to form micelles, and 10:0-LPC/18:2-18:2-PC mixtures are predicted to form micelles or bilayers, respectively. (**b**) Transacylations reached the equilibrium state after about 30 min. Time progression is shown of the reaction between 80 nmol of 14:0-LPC and 20 nmol of either 18:3-18:3-PC or 14:0d-14:0d-PC (14:0d, deuterated 14:0). (**c**) The

concentration of 14:0-18:3-PC at equilibrium depends on the amount of enzyme. 18:3-18:3-PC and 14:0-LPC (2:8) reacted in the presence of different amounts of dTAZ. Saturation was reached at 40 μg dTAZ, corresponding to 1 molecule of enzyme per 200 molecules of substrate. (**d**) Transacylation is promoted by unsaturation and short acyl chains. A series of C18 PC species was incubated either with 14:0-LPC or with 19:0-LPC (PC:LPC=2:8), and newly formed PC species were measured. (**e**) Only 18:1 but not 18:0 is transferred from 18:0-18:1-PC to 19:0-LPC. The mass spectra show transacylation products formed from 80 nmol 19:0-LPC and 20 nmol 18:0-18:1-PC. Two PC isomers were tested, having either 18:0 in sn-1 position and 18:1 in sn-2 position (18:0-18:1) or vice versa (18:1-18:0). In either case, only 18:1 was transferred, forming 19:0-18:1-PC but not 19:0-18:0-PC. (**f**) Tafazzin forms 14:0-14:0d-PC from 14:0-LPC and 14:0d-14:0d-PC (PC:LPC=2:8). Mass spectra show PC species in the presence (dTAZ) or absence (None) of enzyme. Note that the substrate 14:0d-14:0d-PC consists of several species each having a different number of deuterium atoms.

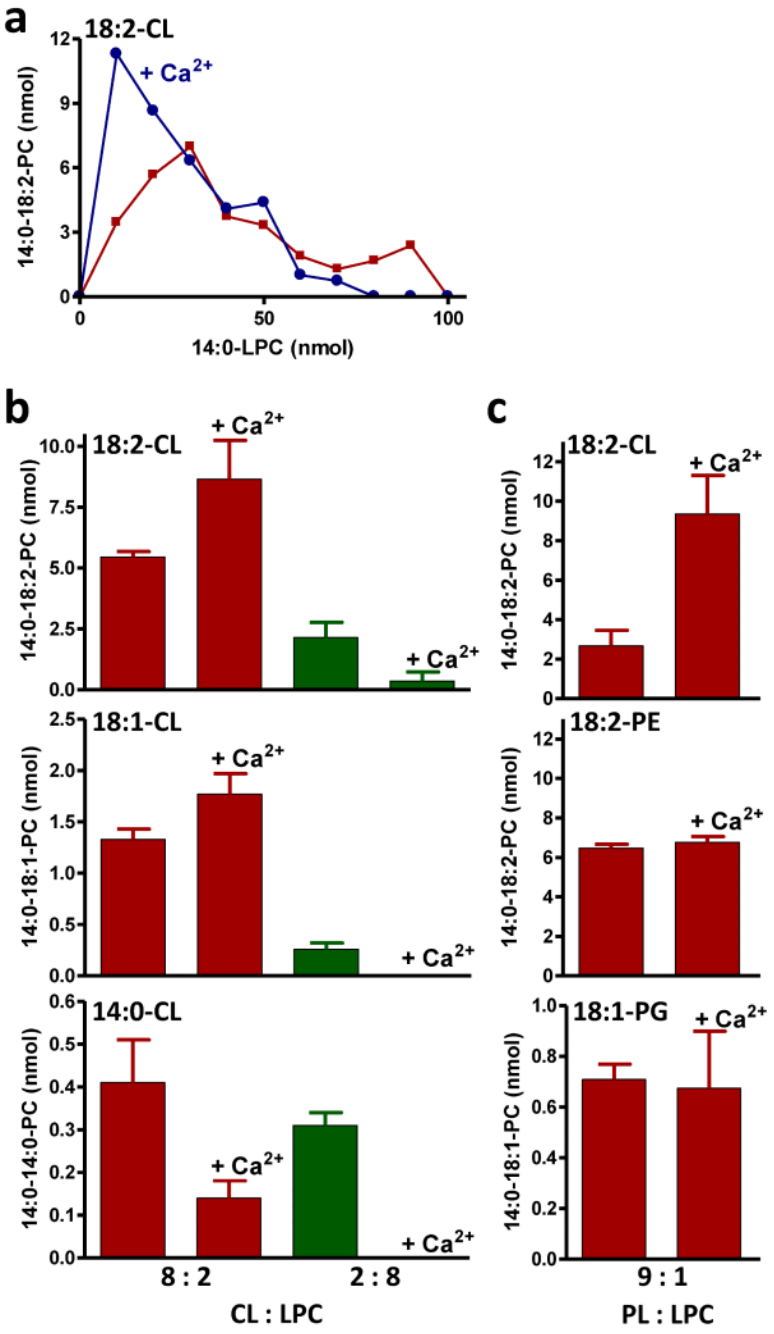

Figure 3. Transacylations of CL but not of PE and PG are affected by Ca^{2+}

Incubations were performed in the presence of purified tafazzin, 14:0-LPC, and the indicated PL with or without 20 mM $CaCl_2$. The proportion of PL and LPC was varied while keeping the total amount of lipids at 100 nmol. (**a**) Ca^{2+} increases CL-LPC transacylation at low LPC concentration and decreases CL-LPC transacylation at high LPC concentration. (**b**) The effect of Ca^{2+} depends on the acyl groups of CL. (**c**) Ca^{2+} has an effect on CL-LPC transacylation but not on PE-LPC and PG-LPC transacylation.

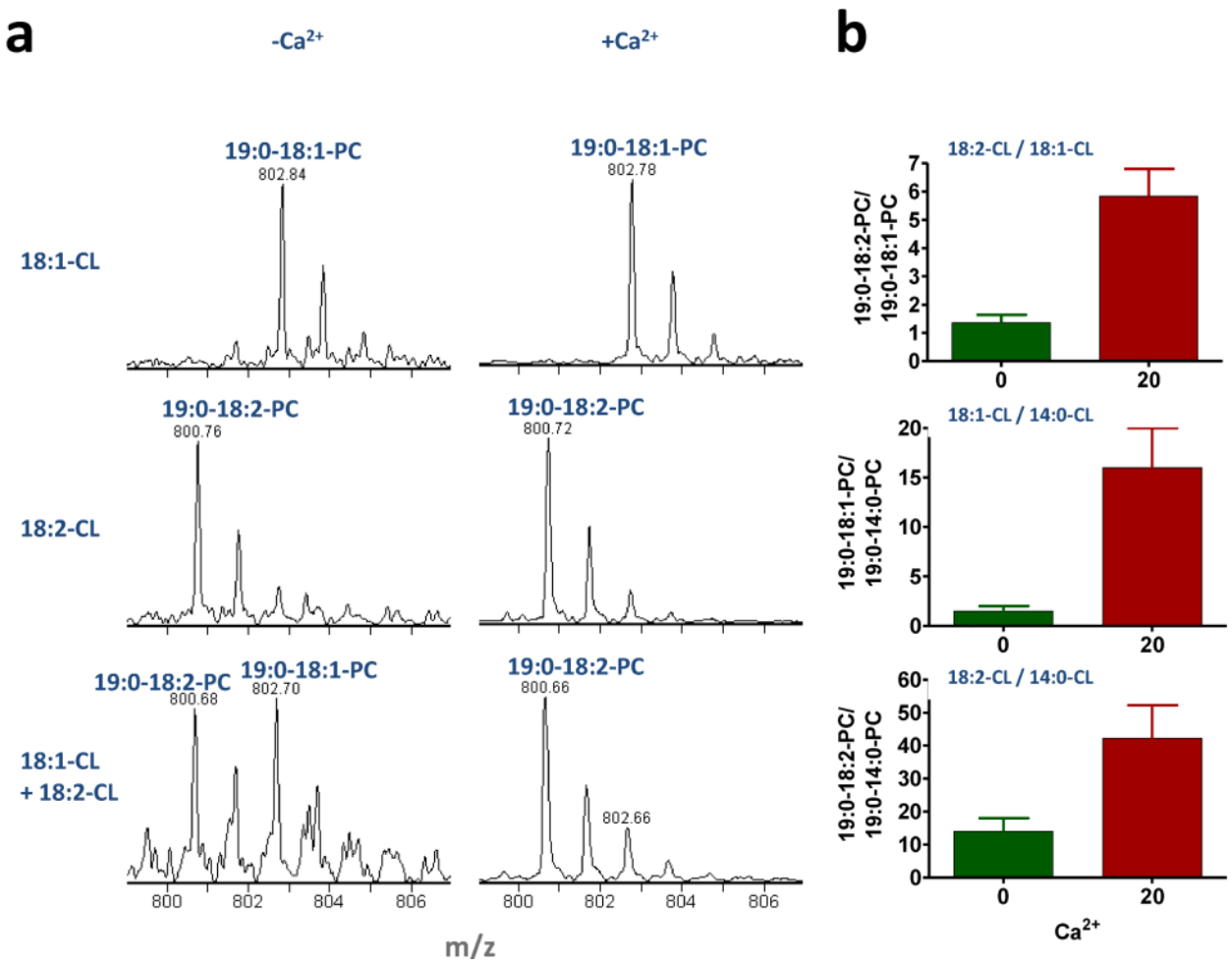

Figure 4. Transition into the hexagonal phase state induces acyl specificity

Incubations contained purified tafazzin, CL (various molecular species), and 19:0-LPC (CL:LPC=9:1). Mixtures of two CL species were supplied at a molar ratio of 1:1. $CaCl_2$ was added at a concentration of 20 mM in order to convert lipids to the hexagonal phase. (**a**) Mass spectra demonstrate the composition of PC species produced by transacylation. In the presence of Ca^{2+}, the transacylation becomes 18:2-specific. (**b**) Bar graphs show the ratios of PC species formed by the indicated pairs of CL species in the absence and presence of Ca^{2+}. The data document that addition of Ca^{2+} alters acyl specificity.

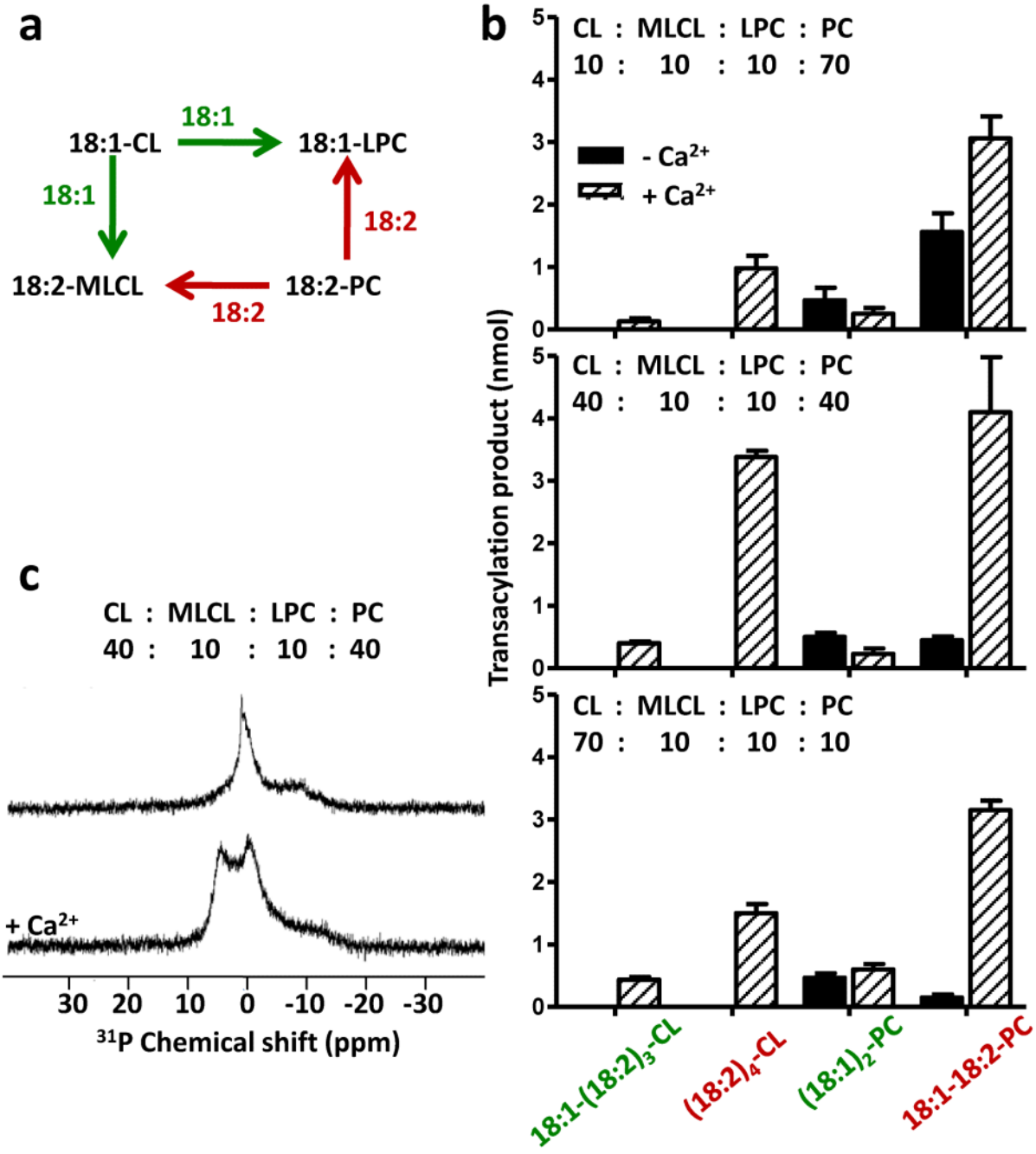

Figure 5. Acyl-specific CL-PC remodeling *in vitro*

Model membranes were produced from a mixture of $(18:1)_4$-CL, $(18:2)_3$-MLCL, 18:1-LPC, and $(18:2)_2$-PC in various proportions. Lipids were sonicated in aqueous buffer with and without $CaCl_2$ followed by incubation in the presence of tafazzin. (**a**) The scheme shows the competing transacylation reactions of this experiment. Linoleoyl groups (18:2) can be transferred from PC to MLCL producing $(18:2)_4$-CL, or from PC to LPC producing 18:1-18:2-PC. Oleoyl groups (18:1) can be transferred from CL to MLCL producing 18:1-$(18:2)_3$-CL, or from CL to LPC producing $(18:1)_2$-PC. (**b**) The bar graphs show the yields of four transacylation products formed either in the absence (black columns) or in the presence (hatched columns) of $CaCl_2$. A complete list of all transacylation products is shown in

Supplementary Table 3. (**c**) Static ^{31}P NMR spectra were recorded of a mixture of $(18:1)_4$-CL, $(18:2)_3$-MLCL, 18:1-LPC, and $(18:2)_2$-PC (40: 10: 10: 40). In the absence of Ca^{2+}, the line shape indicates a phase that is primarily lamellar (low field shoulder). Addition of Ca^{2+} reversed the peak asymmetry, suggesting that a significant portion of the lipids were now in the hexagonal phase. Both the lamellar and the hexagonal phase contained an additional component with isotropic characteristics and a chemical shift close to 0 ppm.

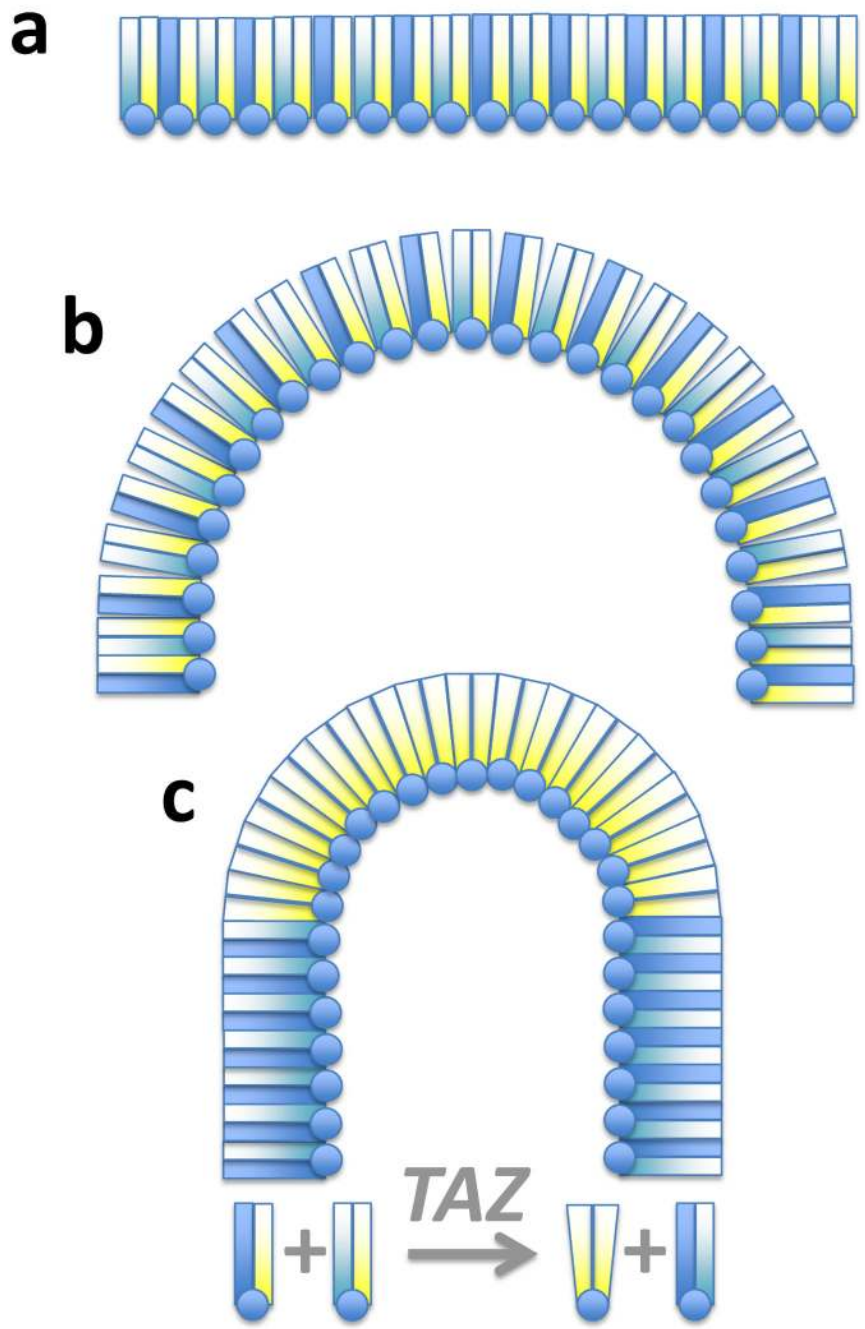

Figure 6. Tafazzin and lipid packing

The cartoon shows our current model of how tafazzin acts on mitochondrial membranes. (**a**) Bilayer-prone PLs form stable arrangements of tightly packed lipid molecules. PL head groups are depicted as circles and fatty acids as color-coded rectangles. Blue and cyan represent saturated residues and yellow represents unsaturated residues. Only one leaflet of the lipid bilayer is shown. (**b**) Bending of the membrane will disturb the packing order of bilayer PLs, which is thermodynamically unfavorable but may facilitate intermixing with LPLs, a requirement for the tafazzin reaction. (**c**) In the presence of tafazzin (TAZ), transacylations will reshuffle the acyl residues in order to optimize lipid packing. In this example, diunsaturated PLs (yellow-yellow) are formed because they promote negative

curvature due to their shape. We propose that highly curved membranes promote the reaction of tafazzin and tafazzin, in turn, stabilizes curvature.

Table 1

Abundance of tafazzin and of endogenous phospholipids reacting with tafazzin in isolated mitochondria

Mitochondria	dTAZ[a] (pmol/mg protein) Mean±SEM, N=3	^{14}C-PC[b] (nmol/mg protein) Mean±SEM, N=3	^{14}C-PC /dTAZ
Drosophila, wild-type	1.1±0.1	0.82±0.23	745
Sf9 cells, moderate dTAZ expression	20±3	1.69±0.31	85
Sf9 cells, high dTAZ expression	86±2	4.38±1.02	51

[a] Drosophila tafazzin

[b] formed from ^{14}C-LPC, represents the amount of endogenous PLs reacting with tafazzin

Table 2

Parameters of PL/LPL mixtures determined by magic angle spinning ^{31}P NMR spectroscopy

PL/LPL mixture[a] (mol : mol)	Isotropic chemical shift (ppm)	Relative peak area (%)	CSA (ppm)	Line width (Hz)	Phase characteristics
PC	−1.28	100	18	679	Lamellar
PC/LPC (8:2)	−5.57	21	2.7	1387	Lamellar
	−0.70	79	17	497	
PC/LPC (2:8)	−0.82	22	0	26	Isotropic
	−0.37	78	0	17	
PE	−0.12	100	−9.9	63	Hexagonal
PE/LPC (9:1)	−0.11	100	−3.9	66	Non-lamellar
PE/LPC (2:8)	−0.27	48	5.2	82	Non-lamellar
	0.41	52	−7.4	589	
CL	0.40	100	17	131	Lamellar
CL/LPC (9:1)	−1.79	22	−11	300	Lamellar + Non-lamellar
	0.07	78	7.9	340	
CL/LPC (8:2)	−0.27	7	−4.9	129	Lamellar + Non-lamellar
	−0.11	63	−9.8	745	
	0.29	30	15	153	
CL/LPC (2:8)	−0.29	59	0	29	Isotropic
	0.20	41	0	41	
CL + Ca^{2+}	−2.35	100	−16	104	Hexagonal
CL/LPC (8:2) + Ca^{2+}	−2.16	100	−13	125	Hexagonal
CL/LPC (2:8) + Ca^{2+}	−0.91	67	−0.05	174	Isotropic
	−0.50	33	0	35	

[a] lipids include 18:2-18:2-PC, 18:2-18:2-PE, bovine heart CL [predominantly (18:2)$_4$-CL], and 14:0-LPC